Functional magnetic resonance imaging of cortical sensitivity to the binaural-level characteristics of high-frequency Gabor click trains.

G. Christopher Stecker and Susan A. McLaughlin
Dept. of Speech and Hearing Sciences
University of Washington

UNIVERSITY OF WASHINGTON

#875

Background

Multiple markers approach to differentiating auditory cortical (AC) fields physiologically (e.g., Bizley et al. 2005, Stecker et al. 2005, Harrington et al. 2008)
Binaural level sensitivity: key dimension for characterizing AC neurons (Zhang et al. 2004, Kitzes 2008)
Goal: use binaural level sensitivity of BOLD (blood-oxygen-level-dependent) response to differentiate AC fields in humans

Objective

Measure sensitivity of AC BOLD response to binaural level characteristics of stimuli
Parametric variation of average binaural level (ABL) , interaural level difference (ILD)

Stimulus presentation

4000 Hz (carrier frequency) Gabor click trains, 3-ms interclick interval (ICI)
Presentation rate: 5 trains of 32 clicks / second ("slow") or 40 trains of 4 clicks ("fast") / second
Level assigned independently at each ear [55-85 dB SPL or silent (-10 dB)]
Presented via piezoelectric insert earphones (Sensimetrics) in ear defenders
Task: detect rare (once per ~13s) presentation of 2-ms ICI by button press

Block design

12-second blocks present binaural level combination x rate
Silent blocks (-10 dB SPL to each ear) occur every 4th block
Image acquired at end of each block (sparse acquisition)
3 runs of 57 blocks per subject

Imaging methods

BOLD echoplanar imaging (Philips, 3 Tesla)
Sparse imaging (TR = 12s, one frame per block)
32 slices (4.5 mm thick), 3mm x 3mm in-plane resolution

Binaural Level Combinations

Right-ear level (dB SPL)

Left-ear level (dB SPL)	-10	55	60	65	70	75	80	85
85	×	×			×			×
80			×				×	
75				×		×		
70	×				×			×
65				×		×		
60			×				×	
55	×	×						×
-10	×	×			×			×

Binaural level combinations presented to subjects are indicated by "x" in the corresponding cell. Shading illustrates sequences used for testing sensitivity to ABL (shades of blue) and ILD (red to green).

Analytical methods

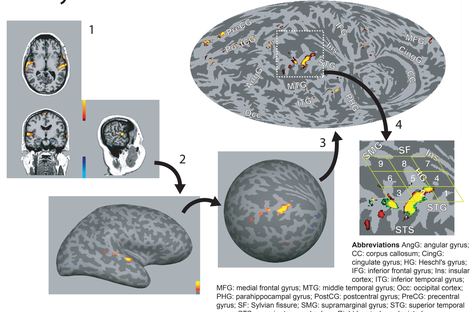

Abbreviations AngG: angular gyrus; CC: corpus callosum; CingG: cingulate gyrus; HG: Heschl's gyrus; IFG: inferior frontal gyrus; Ins: insular cortex; ITG: inferior temporal gyrus; MFG: medial frontal gyrus; MTG: middle temporal gyrus; Occ: occipital cortex; PHG: parahippocampal gyrus; PostCG: postcentral gyrus; PreCG: precentral gyrus; SF: Sylvian fissure; SMG: supramarginal gyrus; STG: superior temporal gyrus; STS: superior temporal sulcus. Right hemisphere depicted.

1) 3-D functional preprocessing with FSL
Motion correction, high-pass filtering (100s)

2) Cortical surface extraction using Freesurfer
Between-subject alignment via sphere
At left, light gray: positive curvature (gyri), dark gray: negative curvature (sulci)

3) Projection to equal-area map (Mollweide)
Center on HG x STG, STG on equator
1mm x 1mm grid, no spatial smoothing

4) Definition of 9 regions of interest
3 x 3 oblique arrangement
Oriented along HG (L-M), STG (A-P)
ROI 1 = anterolateral, ROI 9 = posteromedial

5) Statistical analyses in MATLAB
ANOVA contrasts (1 df)
Percent signal change
Parametric average response

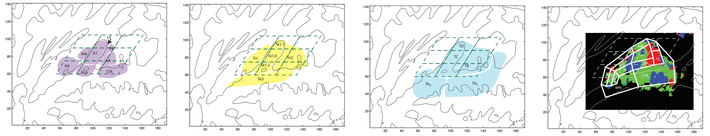

Rough comparison of analytical ROIs (3x3 oblique grid) to parcellation models of human AC. Left to right: based on anatomical observations of Rivier and Clark (1997, violet), Morosan et al. (2001, yellow), and von Economo and Koskinas (1925, blue). Far right: based on comparison of tonotopic organization of AC BOLD responses in Human (Woods et al., in press; red=high frequency, blue = low frequency) and Macaque AC (Kayser et al. 2007). Solid contour line indicates zero curvature. Left hemispheres depicted.

Individual variation in binaural interaction across AC

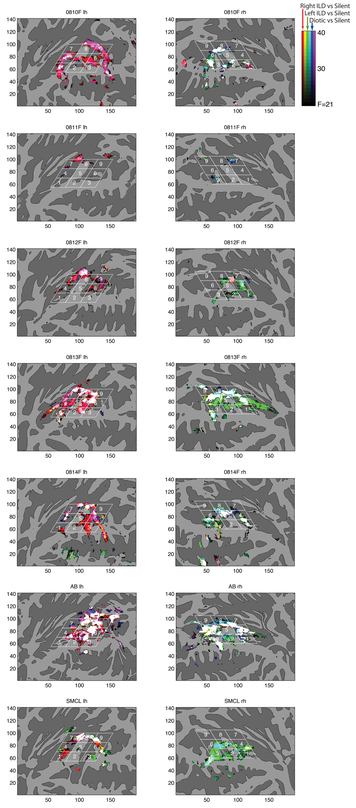

Individual contrast maps reveal contralateral bias, variation in binaural interaction type across cortical surface. Color values plot F statistic (scale at top right), thresholded at $p<10^{-5}$, for simple contrasts: diotic vs silence (blue), left-favoring ILD vs silence (green), right-favoring ILD vs silence (red). Color mixtures follow RGB model (e.g., cyan = similar response to diotic and left ILD). Responses averaged across rate. Rows represent individual subjects. Left hemispheres plotted in left column, right hemispheres in right. Grid and labels indicate ROI positions relative to individual anatomy.

Response dependence on ABL, ILD, and rate varies across AC

Binaural response pattern. Color values plot % signal change, averaged across subjects, for 85 dB SPL vs silence under monotic-left (green), monotic-right (red), and diotic (blue) presentation. Labels, grid indicate ROI positions. Left and right panels plot left and right AC, respectively.

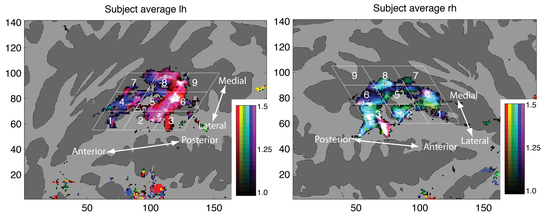

Response-ABL Function

Response-ABL functions. Lines plot percent signal change as a function of ABL for fast (40/s, blue), slow (5/s, red), and combined (black) presentation rates. Panels correspond to ROIs located in left (left panels) and right (right panels) AC. Note variation in overall response magnitude, sensitivity to rate, ABL.

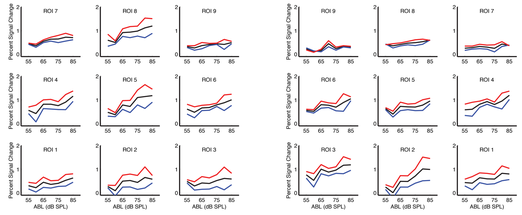

Response-ILD Function

Response-ILD functions. Lines plot percent signal change as a function of ILD. Formatting identical to Response-ABL function, above. Note variation in ILD response profile between ROIs. Also note exaggerated sensitivity to rate at some ILD values.

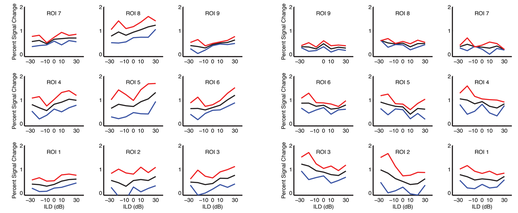

Level-Response Area

Level-response area. Color (blue to red) plots normalized signal change as a function of stimulation level in the right (x-axis) and left (y-axis) ears. White dots indicate tested level combinations; other values interpolated. Dark blue bars separate responses to monotic stimulation (one ear at -10 dB) from rest of plot.

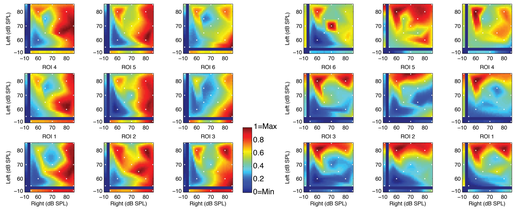

Variation of individual response-ILD functions

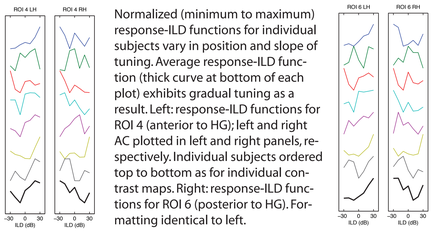

Normalized (minimum to maximum) response-ILD functions for individual subjects vary in position and slope of tuning. Average response-ILD function (thick curve at bottom of each plot) exhibits gradual tuning as a result. Left: response-ILD functions for ROI 4 (anterior to HG); left and right AC plotted in left and right panels, respectively. Individual subjects ordered top to bottom as for individual contrast maps. Right: response-ILD functions for ROI 6 (posterior to HG). Formatting identical to left.

Discussion

1) Variation in binaural level sensitivity across AC?
-Different binaural interaction types (EE / E0 / EI) ?
-AC regions differ in strength of preference for contralateral ear
-Level response area (LRA) can potentially discriminate EI-type ILD tuning from E0-type contralateral drive

2) ROI Determination
-Match size/shape to responses (avoid averaging smaller-scale structures)
-Alignment with functional markers of microanatomy rather than gyral structure
-Accounting for individual variation

3) Pattern recognition to generate candidate ROI based on consistency of response tuning.

4) Role of carrier frequency
-Expect to activate different regions of AC (e.g., low-frequency A1)
-Shift in binaural sensitivity? (change in slope, shift to ITD?)

References

Bizley JK, Nodal FR, Nelken I, and King AJ (2005) *Cereb. Cortex.* 15(10):1637-53
von Economo C and Koskinas GN (1925) *Atlas of Cytoarchitectonics of the Adult Human Cerebral Cortex*
Harrington IA, Stecker, GC Macpherson EA, and Middlebrooks JC (2008) *Hear Res.* 240(1-2):22-41
Kayser C, Petkov CI, Augath M, Logothetis NK. (2007) *J Neurosci.* 27(8):1824-35.
Kitzes LM (2008) *Hear Res.* 238(1-2):68-76
Morosan P, Rademacher J, Schleicher A, Amunts K, Schormann T, and Zilles K (2001) *NeuroImage* 13(4):684-701
Rivier F and Clarke S (1997) *Neuroimage* 6(4):288-304
Stecker GC, Harrington IA, Macpherson EA, and Middlebrooks JC (2005) *J Neurophysiol.* 94(2):1267-80
Woods DL, Stecker GC, Rinne T, Herron TJ, Cate AD, Yund EW, Liao I, and Kang XJ (in press) *PLoS Biology*
Zhang J, Nakamoto KT, and Kitzes LM (2004) *J Neurophysiol.* 91(1):101-17

Acknowledgments

The authors thank Jeff Stevenson and Jenee O'Brien for assistance with scanner configuration and data collection. Work supported by NSF IOB-0630338 and University of Washington.

email: cstecker@u.washington.edu
http://faculty.washington.edu/cstecker